MOF-Supported Selective Ethylene Dimerization Single-Site Catalysts through One-Pot Post-Synthetic Modification

Jerome Canivet, Sonia Aguado, Yves Schuurman and David Farrusseng

1. General remarks

All reactions are carried out in anhydrous solvents. The (Fe)MIL-101-NH_2 is synthesized and activated according to previously reported procedure.[1] All other reagents are commercially available (Sigma-Aldrich) and are used without further purification.
NMR spectra are recorded on a Brüker 250 MHz spectrometer. Chemical shifts are reported in parts per million (ppm) referenced to the appropriate solvent peak. The following abbreviations are used to describe peak patterns when appropriate: s = singlet, d = doublet, q = quadruplet, m = multiplet. However the paramagnetic effect of iron (III), enhanced by the introduction of ~3 wt% of nickel (II) species, does not allow to record NMR spectra under optimal conditions. A very low concentration of the MOF in the deuterated solution is thus required (around 1 $mg.mL^{-1}$), and consequently a high number of scans (ns = 128), in order to get workable spectra.
The XRD measurements on the materials are carried out by powder X-ray diffraction (PXRD) using a Bruker D5005 diffractometer equipped with a secondary graphite monochromator and a scintillation counter.
N_2 isotherms at 77K are performed using a BELSORP-max (BEL Japan).

2. One-pot synthesis of Ni@(Fe)MIL-101

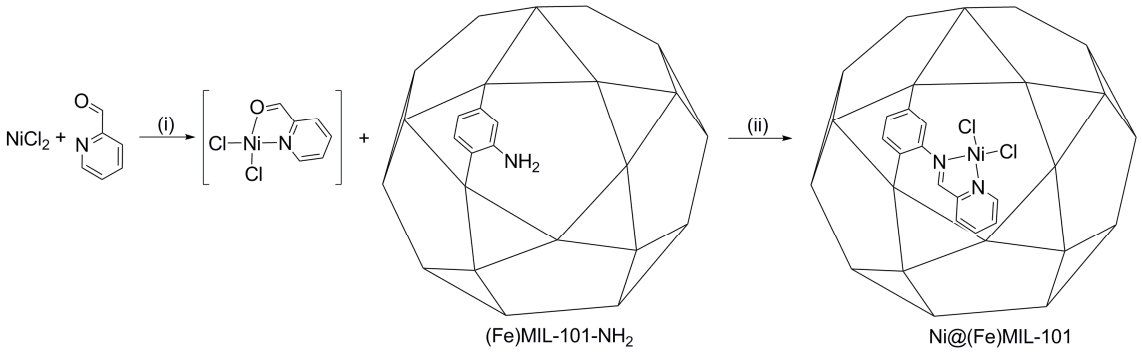

<u>30Ni@(Fe)MIL-101</u>
(i) In a 7 mL glass vial, 141 mg of $NiCl_2 \cdot 6\ H_2O$ (0.6 mmol) are dried with a heatgun under vacuum and kept under argon after cooling to room temperature. Then 3 mL of anhydrous methanol are added, followed by 57 µL of 2-pyridine carboxaldehyde (0.6 mmol). The mixture is stirred at room temperature for one hour to give a clear green solution.
(ii) Then 50 mg of freshly desorbed (Fe)MIL-101-NH_2 (~0.2 mmol -NH_2) are added and the suspension is allowed to react at room temperature for 72 hours. The resulting suspension is centrifuged and the solid washed with methanol (3× 5 mL) and dichloromethane (3× 5 mL) to give the desired product as a fine brown powder after drying under vacuum. Following this procedure, around 30 % of the amino groups are converted into the corresponding imine according to ^{1}H NMR analysis. No 2-pyridine carboxaldehyde remains inside the MOF.
^{1}H NMR (250 MHz, [D6]DMSO-DCl- D_2O) δ 8.77 (1 H, s), 8.62 (1.1 H, s), 8.01-8.11 (2.9 H, m), 7.78-7.95 (3.4 H, m), 7.58-7.65 (3.2 H, m), 7.25-7.38 (3.2 H, m) ppm.

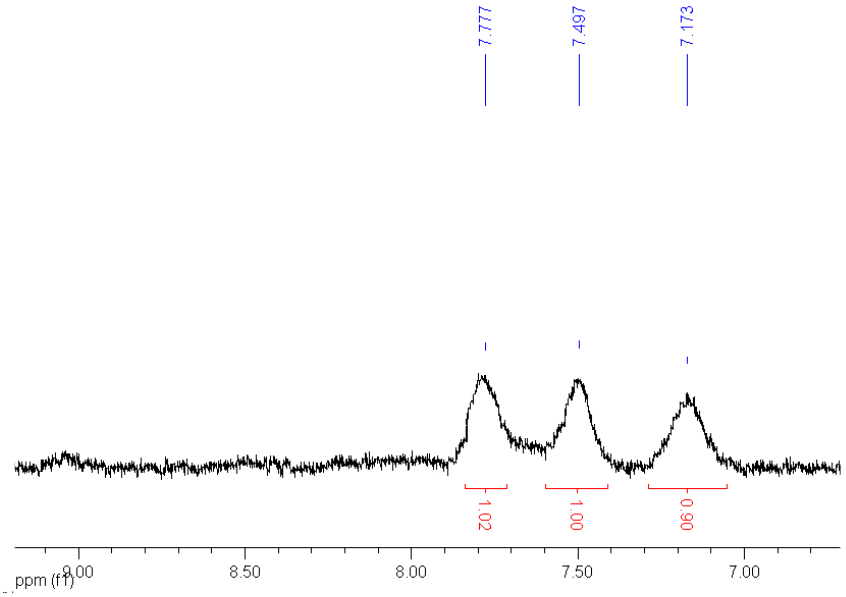

Figure S1. ^{1}H NMR spectrum of digested (Fe)MIL-101-NH_2

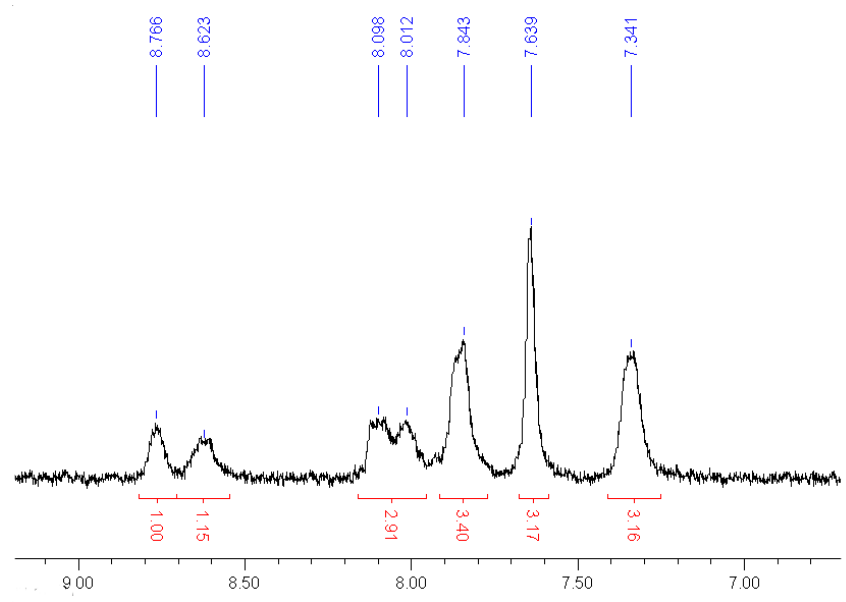

Figure S2. ^{1}H NMR spectrum of digested 30Ni@(Fe)MIL-101 (c.a. 30% modified)

10Ni@(Fe)MIL-101

The 10% functionalized MOF is obtained following the previously described protocol using 47 mg of $NiCl_2 \cdot 6\ H_2O$ (0.2 mmol) and 19 µL of 2-pyridine carboxaldehyde (0.2 mmol). In this case, the suspension is stirred at room temperature for 24 hours.

^{1}H NMR (250 MHz, [D6]DMSO-DCl- D_2O) δ 8.76 (0.3 H, s), 8.63 (0.3 H, s), 8.02-8.11 (0.9 H, m), 7.78-7.86 (2.6 H, m), 7.45-7.55 (2.7 H, m), 7.12-7.27 (2.8 H, m) ppm.

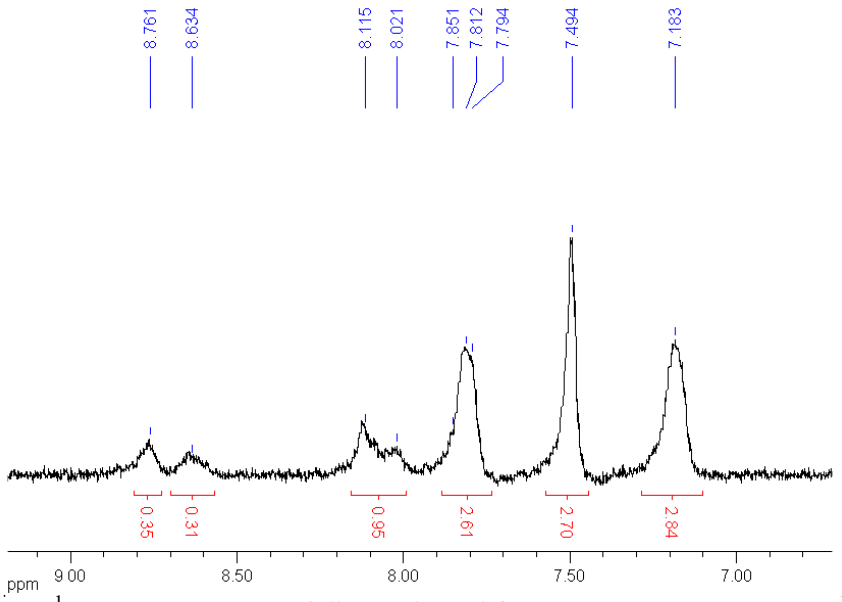

Figure S3. ^{1}H NMR spectrum of digested 10Ni@(Fe)MIL-101 (c.a. 10% modified)

Following the same methodology, reactions using (Cr) MIL-101-NH_2 [2] and (Al) MIL-101-NH_2 [3] were performed. However, these attempts were not successful and no grafting was observed by NMR.

3. X-ray diffraction (XRD)

The XRD measurements on the materials were carried out by powder X-Ray diffraction (PXRD) using a Bruker D8 Advance Diffractometer equipped with a Lyon-Eye detector (CuKα radiation, wavelengths λ = 0.154178 nm). The XRD studies were done at room temperature.

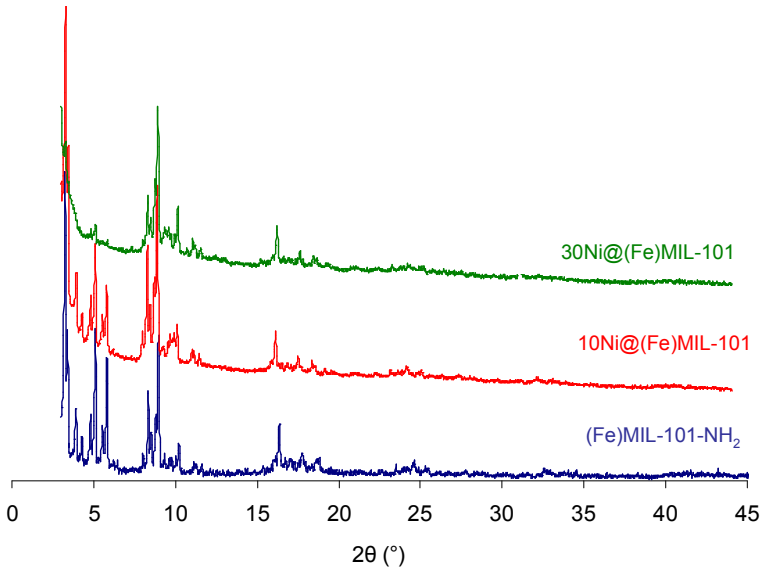

Figure S4. PXRD patterns of (Fe)MIL-101-NH_2 (bottom) and 10Ni@(Fe)MIL-101 (middle) and 30Ni@(Fe)MIL-101 (top).

4. Structural analysis

The structural analysis of functionalized MOFs through transmission electron microscopy (TEM) led to the observation of mainly iron-nickel aggregates into amorphous organic matrix due to the lack of stability of the MOF material under the electron beam.

The surface morphology of the samples were examined by scanning electron microscopy (SEM) using a JSM 5800LV (JEOL), coupled to an analysis system by energy dispersion spectrometry (EDS) with a diode Si-Li (PGT). The tension range is 0.3-30 kV and the effective resolution is 0.5 nm at 30kV.

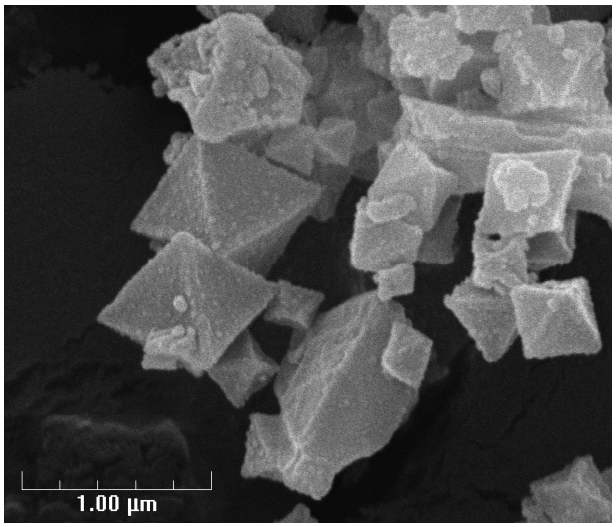

Figure S5. SEM picture of 10Ni@(Fe)MIL-101 crystals.

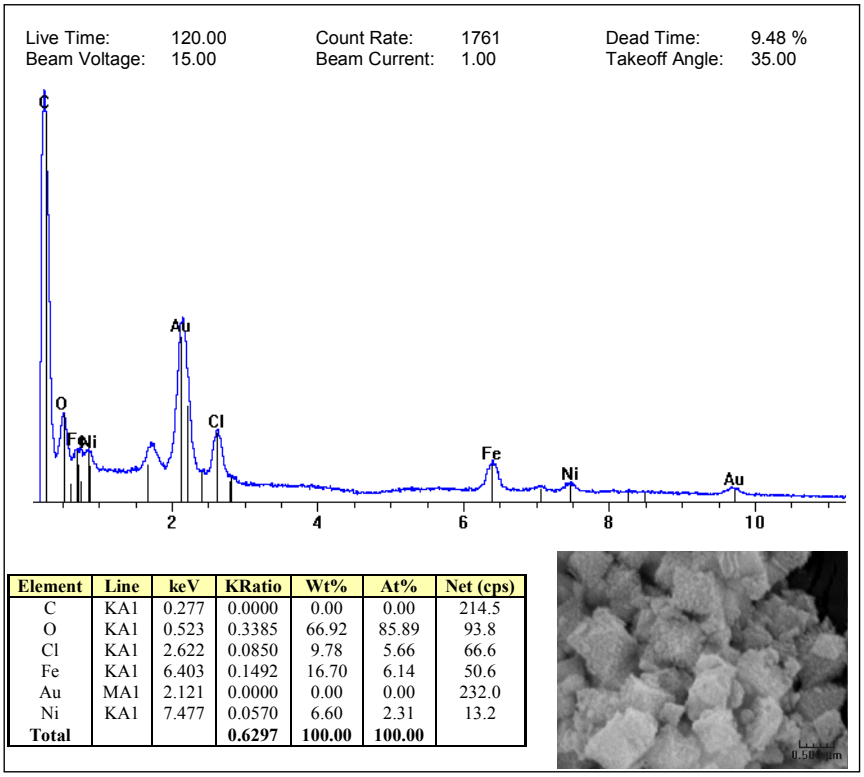

Element	Line	keV	KRatio	Wt%	At%	Net (cps)
C	KA1	0.277	0.0000	0.00	0.00	214.5
O	KA1	0.523	0.3385	66.92	85.89	93.8
Cl	KA1	2.622	0.0850	9.78	5.66	66.6
Fe	KA1	6.403	0.1492	16.70	6.14	50.6
Au	MA1	2.121	0.0000	0.00	0.00	232.0
Ni	KA1	7.477	0.0570	6.60	2.31	13.2
Total			**0.6297**	**100.00**	**100.00**	

Figure S6. EDS analysis of 30Ni@(Fe)MIL-101

Elements ratio calculated for $Fe_3OCl(BDC\text{-}NH_2)_2[(BDC\text{-}NCHPy)NiCl_2]$: Fe:Ni:Cl = 3 : 1 : 3, Found: Fe:Ni:Cl = 3 : 1.2 : 2.8.

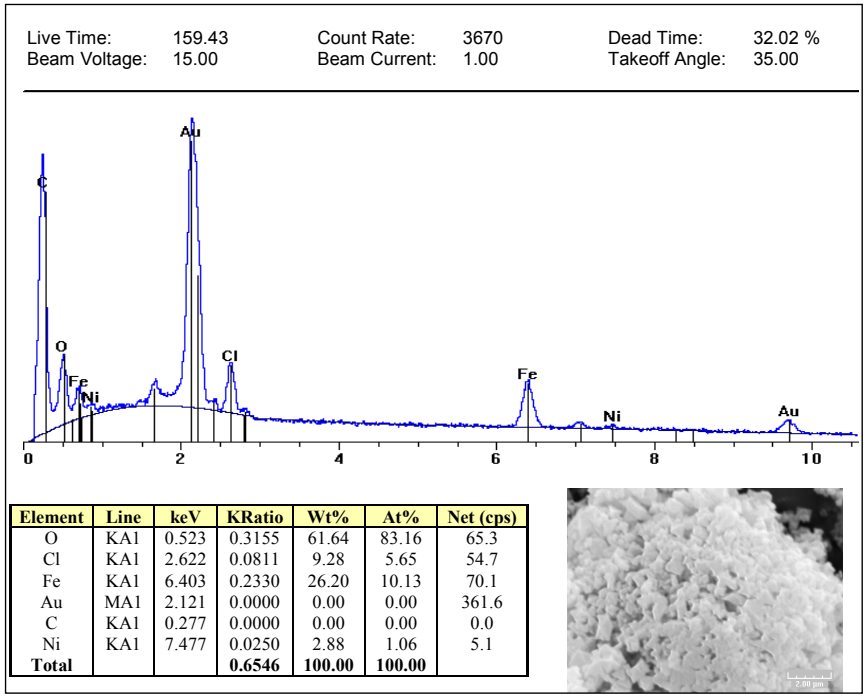

Element	Line	keV	KRatio	Wt%	At%	Net (cps)
O	KA1	0.523	0.3155	61.64	83.16	65.3
Cl	KA1	2.622	0.0811	9.28	5.65	54.7
Fe	KA1	6.403	0.2330	26.20	10.13	70.1
Au	MA1	2.121	0.0000	0.00	0.00	361.6
C	KA1	0.277	0.0000	0.00	0.00	0.0
Ni	KA1	7.477	0.0250	2.88	1.06	5.1
Total			**0.6546**	**100.00**	**100.00**	

Figure S7. EDS analysis of 10Ni@(Fe)MIL-101

Elements ratio calculated for $Fe_3OCl(BDC\text{-}NH_2)_{2.7}[(BDC\text{-}NCHPy)NiCl_2]_{0.3}$: Fe:Ni:Cl = 3 : 0.3 : 1.6, Found: Fe:Ni:Cl = 3 : 0.31 : 1.67.

5. Gas sorption analyses

The N_2 adsorption/desorption isotherms at 77 K were measured on a BELSORP-MAX. The samples were outgassed under vacuum (~ 10^{-4} mbar) at 393K for 12 h before start of the measurements. The specific surface was determined by BET method.

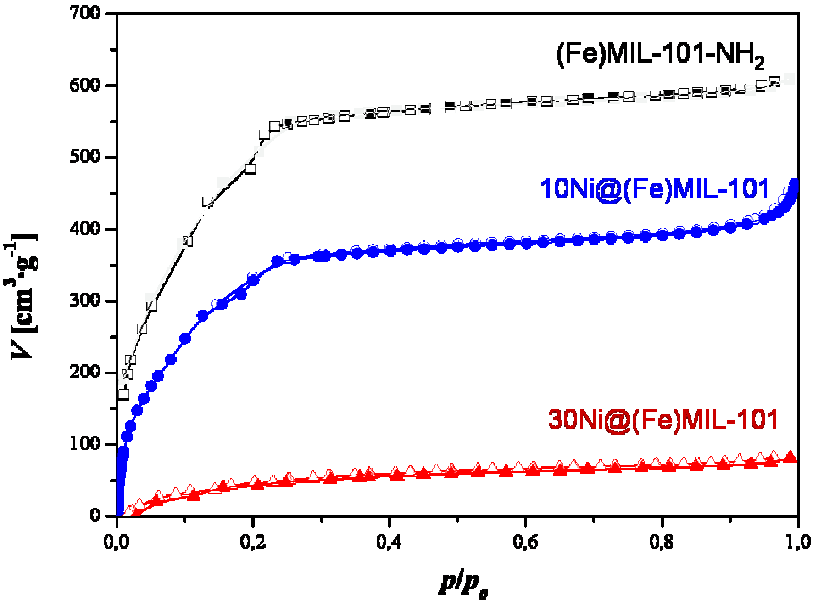

Figure S8. Nitrogen isotherms (77 K) represented as linear-linear diagrams for (Fe)MIL-101-NH_2 (■), 10Ni@(Fe)MIL-101 (●) and 30Ni@(Fe)MIL-101 (▲). Close and open symbols correspond to adsorption and desorption data, respectively.

MOF	BET surface area (m^2/g)
(Fe)MIL-101-NH_2	1884
10Ni@(Fe)MIL-101	1110
30Ni@(Fe)MIL-101	155

6. Ethylene oligomerization

In a typical catalytic run, 8 mg of 10Ni@(Fe)MIL-101, corresponding to 2.8 μmol of nickel, are introduced into a 30 mL stainless steel autoclave followed by 15 mL of *n*-heptane and 0.2 mL of Et_2AlCl (1M in *n*-heptane, Al/Ni = 70). After degassing three times, the pressure is kept constant at 15 bars with C_2H_4 for one hour. Then the reactor is cooled in an ice bath and cold distilled water is added to quench the reaction. The organic layer kept cold is quickly analyzed by gas chromatography (HP 6890N equipped with a 30 m HP5 column) using heptane signal as reference.
Ni(bipy)Cl_2 was prepared according to the published method.[4]

Table S1. Ethylene oligomerization in liquid phase under 15 bars [a]

entry	catalyst (μmol)[b]	T (°C)	intrinsic activity (h^{-1})[c]	selectivity (%)		
				C_4	C_6	C_8
1	none	10	0	n.d.	n.d.	n.d.
2	Ni(PPh_3)$_2Cl_2$ (35)	10	9540	84	15.6	0.4
3	Ni(bipy)Cl_2 (35)	10	175	92	8	0
4	Ni(bipy)Cl_2 (2.8)	10	210	92	7.5	0.5
5	(Fe)MIL-101-NH_2[d]	10	0	n.d.	n.d.	n.d.
6	(Fe)MIL-101-NH_2 + $NiCl_2$ (35)[e]	10	0	n.d.	n.d.	n.d.
7	30Ni@(Fe)MIL-101 (8.4)	10	3215	94	5.5	0.5
8	10Ni@(Fe)MIL-101 (2.8)	0	6	n.d.	n.d.	n.d.
9	10Ni@(Fe)MIL-101 (2.8)	10	3166	95	4.5	0.5
10	10Ni@(Fe)MIL-101 (2.8)[f]	10	3085	94	5	1
11	10Ni@(Fe)MIL-101 (2.8)[g]	10	2972	94.5	4.5	1
12	10Ni@(Fe)MIL-101 (2.8)	20	4705	89.3	9.5	1.2
13	10Ni@(Fe)MIL-101 (2.8)	30	1800	93	6.5	0.5
14	10Ni@(Fe)MIL-101 (2.8)	40	2	n.d.	n.d.	n.d.

[a] Reaction performed in 15 mL of dry heptane in the presence of Et_2AlCl (Al/Ni = 70); [b] Based on the amount of nickel, corresponding to 8 mg of Ni@(Fe)MIL-101; [c] Estimated by GC analysis of the organic phase and calculated as (moles of oligomer formed)/(moles of Ni · h); [d] Reaction performed using 8 mg of MOF; [e] Reaction performed using 8 mg of MOF and $NiCl_2$ (35 mmol, 4.5 mg); [f] Catalyst reused for a second run; [g] Catalyst reused for a third run.

Table S2. Reported catalytic activity of representative Ni-based materials (Ni-*material*) and supported nickel complexes (Ni@*support*) for the ethylene oligomerization.

catalyst type	**T (°C)**	**$P_{ehtylene}$ (bars)**	**Al/Ni**	**$g_{oligom}/g_{cat}/h$**	**$kg_{oligom}/g_{Ni}/h$**	**$kg_{oligom}/mol_{N}i/h$**	**$mol_{oligom}/mol_{Ni}/h$**	**reference**
Ni@MIL-101	**25**	**30**	**70**	**205**	**10**	**585**	**10455**	this study
Ni-MOF	5	15	70	21	n.a	n.a	n.a	[4]
Ni-PCP	25	12	5	n.a	n.a	n.a	305	[5]
Ni-MCM	150	40	0	66	n.a	n.a	n.a	[6]
[Ni(*N*,*N*)]@silica	60	11.5	2000	n.a	n.a	30000	n.a	[7]
[Ni(*P*,*O*)]@polymer	75	50	0	n.a	0.19	n.a	n.a	[8]
[Ni(*N*,*N*)]@silica or polymer	30	10	400	n.a	n.a	600	n.a	[9]
[Ni(*N*,*N*)]@silica	60	11.5	80	n.a	400	n.a	n.a	[10]
[Ni(*N*,*O*)]@IL	25	0.5	400	n.a	n.a	n.a	45000	[11]

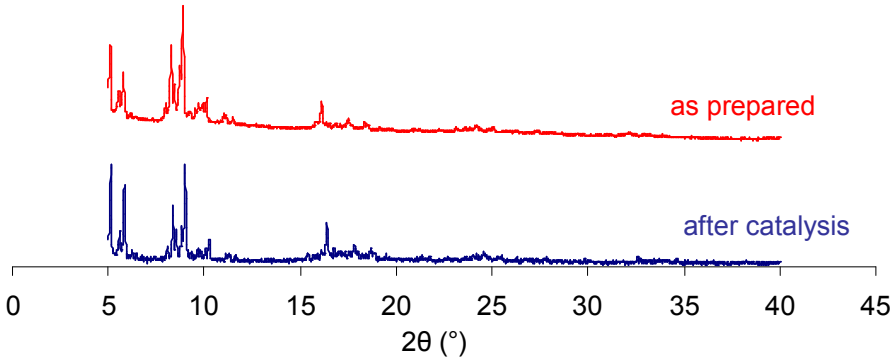

Figure S10. PXRD pattern of 10Ni@(Fe)MIL-101 before (top) and after (bottom) catalytic run.

PXRD data of the sample after catalysis is recorded on a simply washed sample without drastic desorption. Reactants might stack inside the material leading to slight change in peaks intensity or broadening.

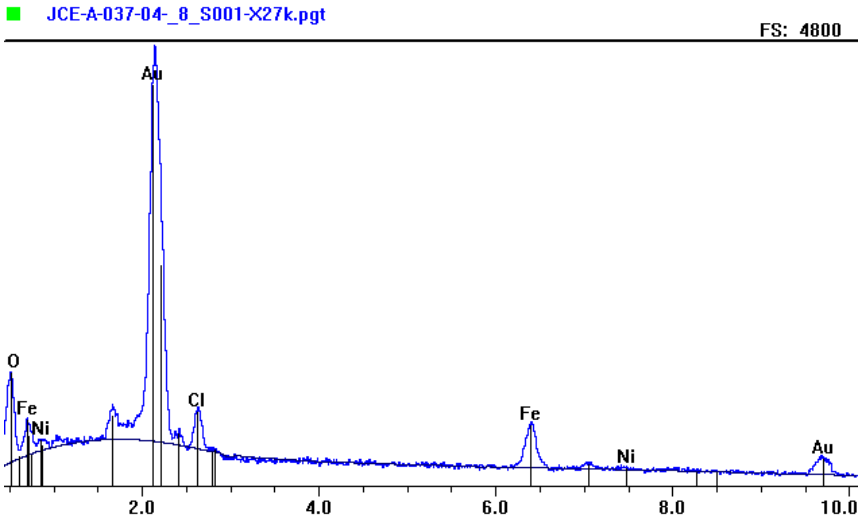

Element	Line	keV	KRatio	Wt%	At%	Net (cps)
O	KA1	0.523	0.4012	68.54	87.35	44.5
Cl	KA1	2.622	0.0449	5.19	3.01	20.1
Fe	KA1	6.403	0.2084	23.82	8.78	33.6
Au	MA1	2.121	0.0000	0.00	0.00	250.6
C	KA1	0.277	0.0000	0.00	0.00	0.0
Ni	KA1	7.477	0.0210	2.45	0.86	2.3
Total			**0.6755**	**100.00**	**100.00**	

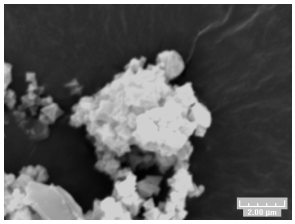

Figure S11. EDS analysis of 10Ni@(Fe)MIL-101 after catalysis

Elements ratio calculated for $Fe_3OCl(BDC\text{-}NH_2)_{2.7}[(BDC\text{-}NCHPy)NiCl_2]_{0.3}$: Fe:Ni:Cl = 3 : 0.3 : 1.6, Found: Fe:Ni:Cl = 3 : 0.29 : 1.03.

The lack of chlorine atoms might be explained by the reaction pathway described in the figure S20 in which nickel species are supposed to lose chlorides.

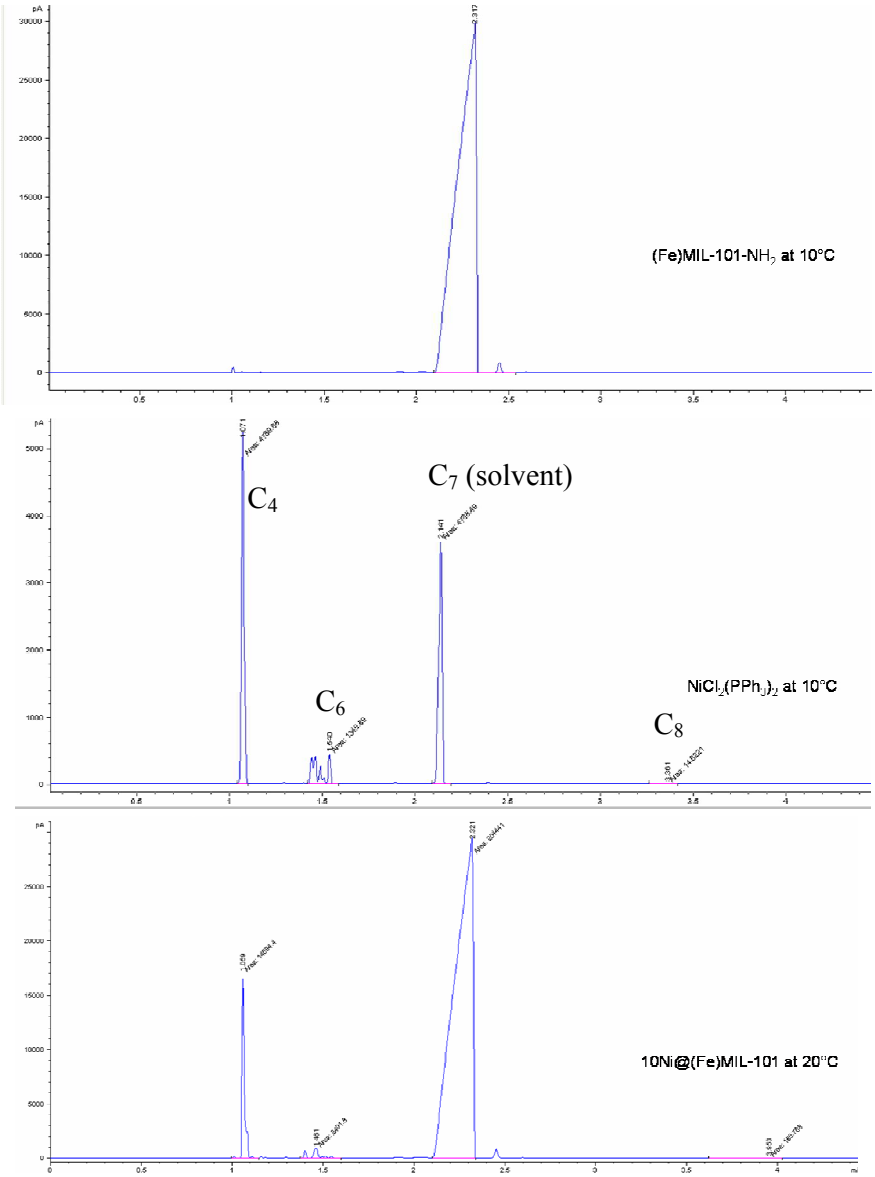

Figure S12. Typical GC traces.

- **Variation of reaction parameters**

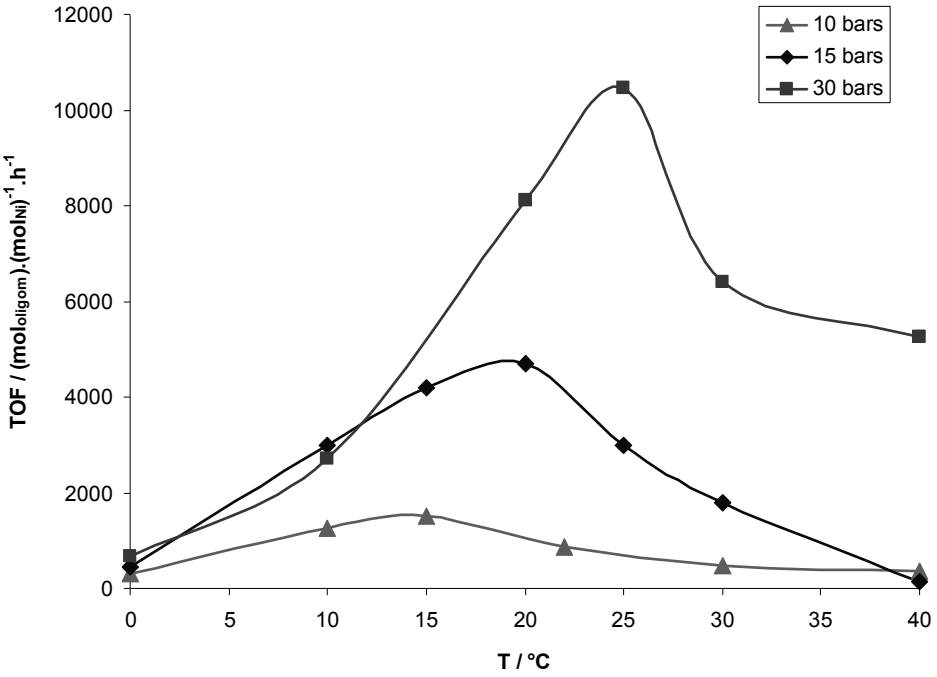

Figure S13. Temperature- and pressure-dependent catalytic activity for 10Ni@(Fe)MIL-101 at 800 rpm and Al/Ni = 70.

- **Products distribution**

The composition of oligomers varies with the activity. When the activity is increasing, the selectivity to butenes slightly decreases.

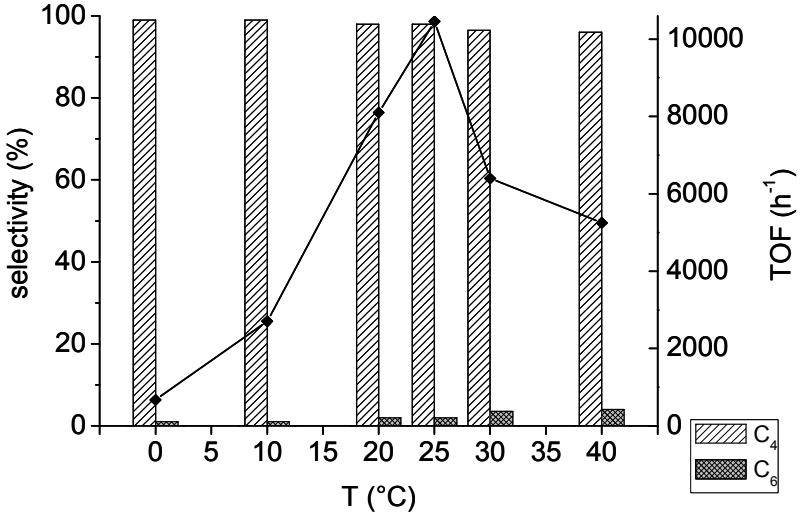

Figure S14. Temperature-dependent oligomers distribution for 10Ni@(Fe)MIL-101 under 30 bars of ethylene .

The C4 – C6 fraction composition was studied by 2-dimensional GC analysis coupled with mass spectrometer:

GC conditons : ZOEX – cryogenic System

- Column 1 : ZB5 - 30m x 0.25mm x 0.25µm
- Column 2 : VF17 - 1.5m x 0.1mm x 0.1µm
- Detection : MS (m/z from 25 to 275)
- Split : 250
- Temp. Program oven 1 : 50°C (5min) then 1.75°C/min to 320°
  oven 2 : 50°C (2min) then 2.10°C/min to 330° (24min)

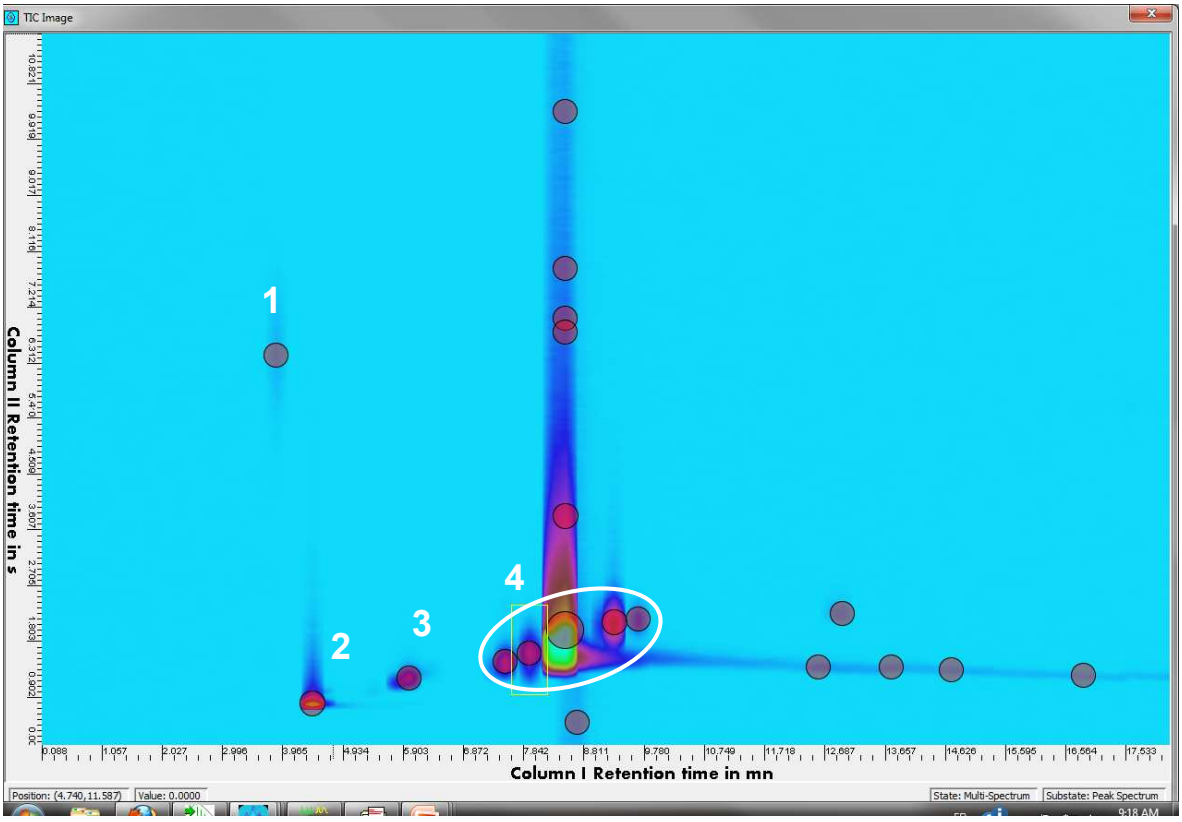

Figure S15. 2-D GC chromatogram obtained for 10Ni@(Fe)MIL-101 at 25°C under 30 bars of ethylene.

peak on the 2D-GC trace	products detected by MS
1	ethylene C2
2	butenes C4
3	hexenes C6
4	heptane C7 from solvent

Only one peak appears for the C4 fraction (number 2, fig. S14) as well as for the C6 (number 3, fig. S14) which shows that no isomerization occurs to form other butenes and hexenes. Varying the amount of Et_2AlCl, no effect of the Al:Ni ratio is observed for values higher than 70.

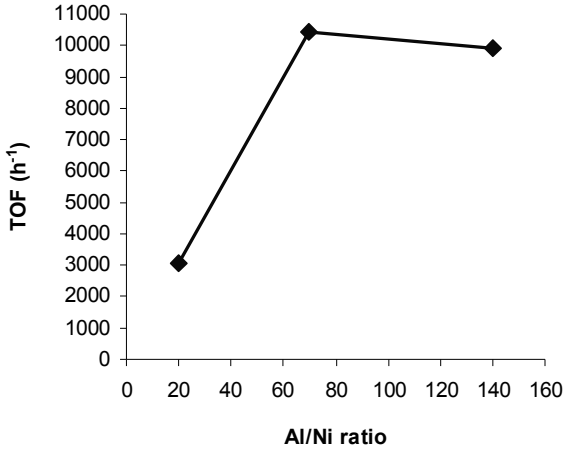

Figure S16. Variation of Al/Ni ratio in the case of 10Ni@(Fe)MIL-101 under 30 bars of ethylene at 25°C and 800 rpm.

The absence of effect of the stirring speed allows determining that the reaction proceeds under kinetic regime, without diffusion limitation.

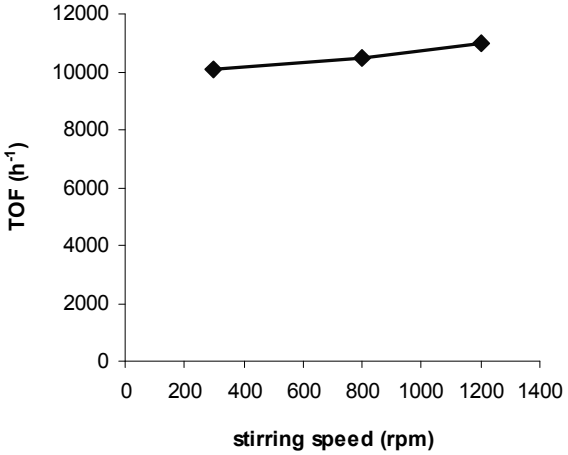

Figure S17. Variation of stirring speed in the case of 10Ni@(Fe)MIL-101 under 30 bars of ethylene at 25°C and Al/Ni = 70.

- **Carbon balance**

In order to follow the ethylene consumption, 16 mg of 30Ni@(Fe)MIL-101, corresponding to 16.8 µmol of nickel, are introduced into a 100 mL stainless steel autoclave equipped with mechanical stirrer. Then 60 mL of *n*-heptane and 1.2 mL of Et_2AlCl (1M in *n*-heptane, Al/Ni = 70) are added. After degassing three times with helium, the pressure of ethylene is kept constant at 15 bars in the reactor thanks to a pressurized tank. The mixture is stirred at 800 rpm, the pressurized tank is at 20°C as well as the reactor.

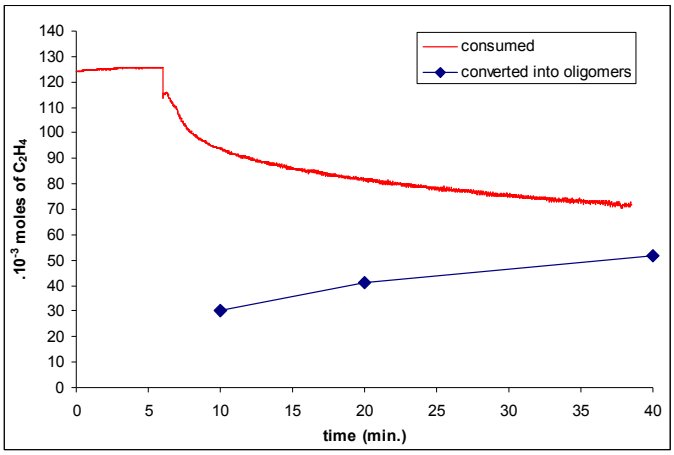

Figure S18. Ethylene consumption from pressure variation (red) and oligomers formation from GC analysis (blue) at 20°C under 15 bars of C_2H_4.

According to the figure S17, each mole of gaseous ethylene is converted into oligomers without loss of carbons.

In order to study the temperature dependence of the catalytic activity, the same experiment has been performed at 40°C. The pressurized tank in this case is still at 20°C when the reactor is heated at 40°C by water circulation.

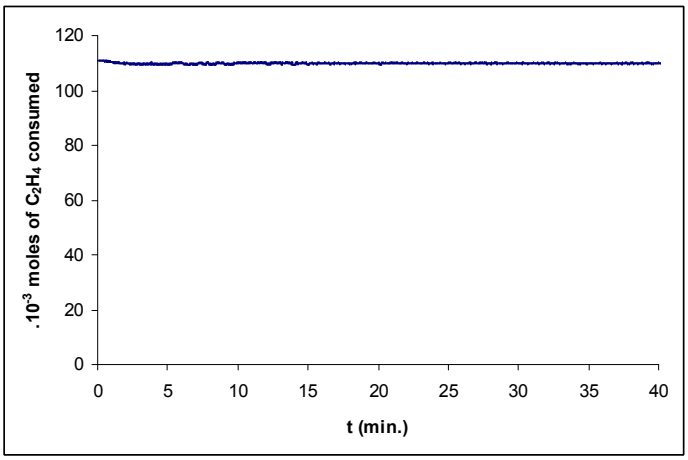

Figure S19. Ethylene consumption from pressure variation at 40°C under 15 bars of C_2H_4.

According to the variation of pressure, $1.3 \cdot 10^{-3}$ moles of ethylene are consumed which is in line with the GC analysis of the catalytic solution. This confirmed the very low catalytic activity at 40°C under 15 bars of ethylene.

- **Kinetic model**

According to the kinetic model, there is a weak contribution of the ethylene solubility to the pressure- and temperature-dependent activity variation.

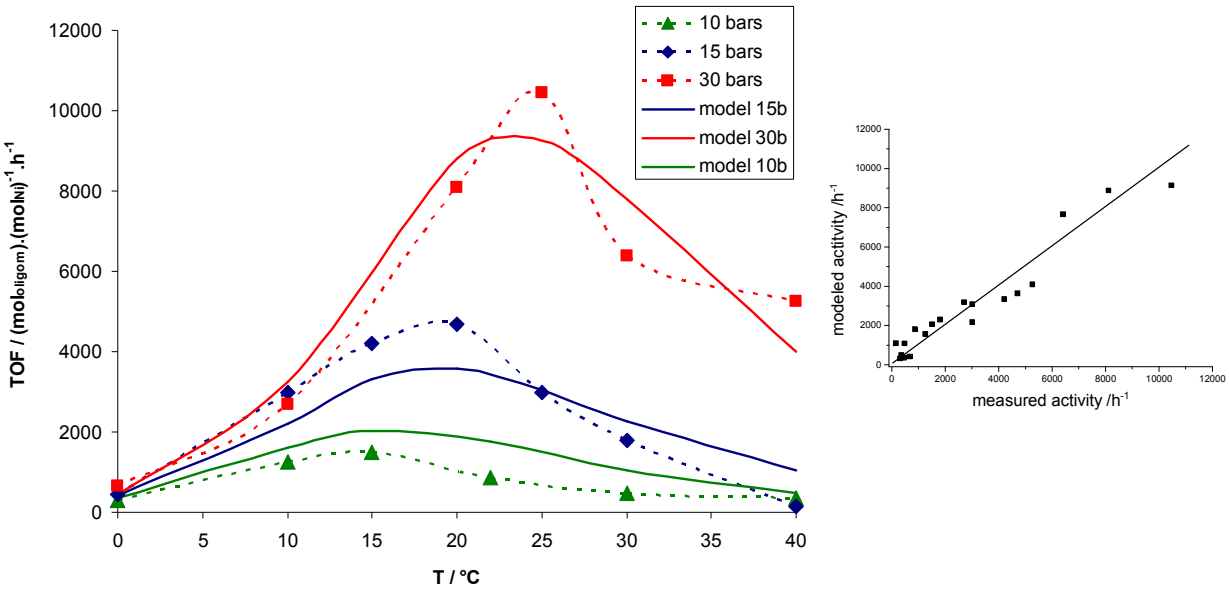

Figure S20. Kinetic model validating temperature- and pressure-dependent activity trend found for 10Ni@(Fe)MIL-101.

The model is based on a reaction mechanism involving the chemisorption of two ethylene molecules on an active nickel site followed by an oligomerization step into 1-butene (Figure S20). The heat of adsorption estimated through this kinetic model is found to be $-\Delta H_{ethylene}$ = 106 ± 18 kJ·mol^{-1} corresponding to carbon-metal bond formation on the activated nickel species. Due to the high activation energy of the oligomerization step (E_{act} = 152 ± 18 kJ·mol^{-1}), the reaction rate increases rapidly with increasing temperature. At the same time the concentration of chemisorbed ethylene molecules decreases with temperature, eventually becoming the dominant process at higher temperatures and lowering the overall rate. The rate of oligomer production, based on competitive ethylene adsorption and the surface reaction as rate-determining step can be written as:

$$r = \frac{N_s k_r^0 \exp\left(\frac{-E_{act}}{RT}\right)\left(K^0_{C_2H_4}\left(\frac{-\Delta H}{RT}\right)C_{C_2H_4}\right)^2}{\left(1+K^0_{C_2H_4}\left(\frac{-\Delta H}{RT}\right)C_{C_2H_4}\right)^2} \quad [\mathrm{mol_{oligom}/mol_{Ni}/h}] \qquad (1)$$

where C_{C2H4} is the ethylene concentration in heptane. The solubility of ethylene in heptane as a function of pressure and temperature has been explicitly taken into account in the model.[12] Its effect on the oligomer production rate is small compared to the effect of the ethylene adsorption on the nickel sites. The parameters, the pre-exponential factor for reaction, k^0_r, the pre-exponential factor for ethylene adsorption, K^0_{C2H4}, as well as E_{act} and ΔH have been estimated by non-linear regression analysis of the all experimental data simultaneously and rate equation (1). A statistical analysis of the parameter estimates after regression showed a

strong correlation between the two pre-exponential factors. The values of the energy parameters are reported above with their 95% confidence intervals. The parity plot of the calculated and experimental data shows no particular deviations.

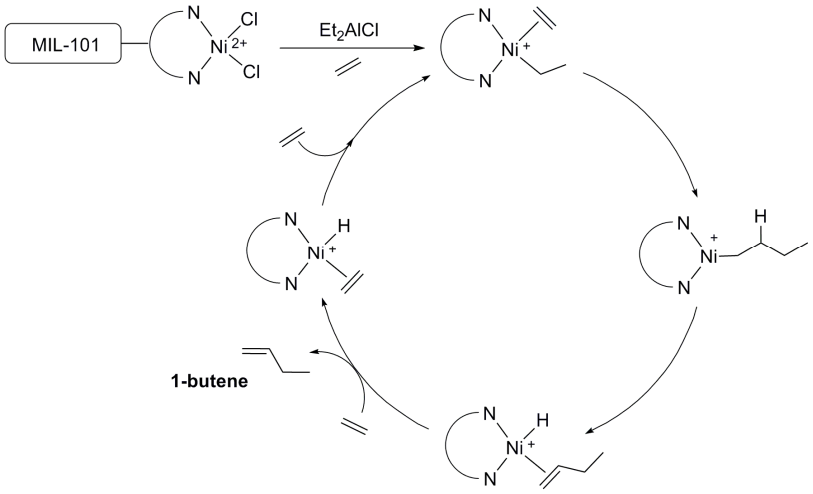

Figure S21. Postulated catalytic cycle for the ethylene dimerization catalyzed by 10Ni@(Fe)MIL-101.

7. References

(1) Bauer, S.; Serre, C.; Devic, T.; Horcajada, P.; Marrot, J.; Ferey, G.; Stock, N. *Inorg. Chem.* **2008**, *47*, 7568.
(2) Bernt, S.; Guillerm, V.; Serre, C.; Stock, N. *Chem. Commun.* **2011**, *47*, 2838.
(3) Hartmann, M.; Fischer, M. *Microporous Mesoporous Mater.* **2012**, *164*, 38.
(4) Kyogoku, K.; Yamada, C.; Suzuki, Y.; Nishiyama, S.; Fukumoto, K.; Yamamoto, H.; Indo, S.; Sano, M.; Miyake, T. *J. Jpn. Petrol. Inst.* **2010**, *53*, 308.
(5) Angelescu, E.; Che, M.; Andruh, M.; Zavoianu, R.; Costentin, G.; Mirica, C.; Pavel, O. D. *J. Mol. Catal. A-Chem.* **2004**, *219*, 13.
(6) Lallemand, M.; Rusu, O. A.; Dumitriu, E.; Finiels, A.; Fajula, F.; Hulea, V. *Appl. Catal., A* **2008**, *338*, 37.
(7) Choi, Y.; Soares, J. B. P. *Macromol. Chem. Phys.* **2009**, *210*, 1979.
(8) Braca, G.; Galletti, A. M. R.; Digirolamo, M.; Sbrana, G.; Silla, R.; Ferrarini, P. *J. Mol. Catal. A-Chem.* **1995**, *96*, 203.
(9) Li, Y.-G.; Pan, L.; Zheng, Z.-J.; Li, Y.-S. *J. Mol. Catal. A-Chem.* **2008**, *287*, 57.
(10) Preishuber-Pflugl, P.; Brookhart, M. *Macromolecules* **2002**, *35*, 6074.
(11) Song, K.-M.; Gao, H.-Y.; Liu, F.-S.; Pan, J.; Guo, L.-H.; Zai, S.-B.; Wu, Q. *Catal. Lett.* **2009**, *131*, 566.
(12) Sahgal, A.; La, H. M.; Hayduk, W. *Can. J. Chem. Eng.* **1978**, *56*, 354.